Early and Delayed Technetium-99m-Tetrofosmin Myocardial SPECT Compared in Normal Volunteers

Ichiro Matsunari, Yoshinobu Tanishima, Junichi Taki, Kouichi Ono, Hiroko Nishide, Susumu Fujino, Munetaka Matoba, Kenji Ichiyanagi and Norihisa Tonami

Department of Radiology, Radioisotope Division and Department of Cardiology, Fukui Prefectural Hospital, Fukui, Japan; and Department of Nuclear Medicine, Kanazawa University School of Medicine, Kanazawa, Japan

This study was performed to test the feasibility of early SPECT imaging with ^{99m}Tc-tetrofosmin with the presence of high hepatic activity. **Methods:** Thirteen normal volunteers were injected 600–740 MBq of ^{99m}Tc-tetrofosmin at rest and were imaged at 10 min and 1 hr after injection. The SPECT images were reconstructed for 180° and 360° data. The early and delayed SPECT and anterior planar projection images were analyzed. **Results:** After excluding one subject because of high hepatic activity overlapping to the myocardium, 4 of 12 subjects (33%) had abnormal scans with reduced uptake in the inferior wall on the early 180° SPECT image. In contrast, only one (8%) showed equivocally reduced uptake on the 360° SPECT image. In the delayed images, all subjects had a normal 180° and 360° SPECT scan. Quantitative data showed reduced regional activities in the inferior wall on the early SPECT scan, especially in the 180° data. There were no changes in the mean anterior-to-inferior ratio in the anterior planar projection images over time, suggesting that the reduced activity in the early SPECT images reflected an artifactual effect. **Conclusion:** Our data indicate that it would be best to perform late imaging in patients with suspected coronary artery disease using ^{99m}Tc-tetrofosmin.

Key Words: technetium-99m-tetrofosmin; myocardial SPECT; liver-heart artifact.

J Nucl Med 1996; 37:1622–1626

Recent phantom studies have demonstrated that an artifactual defect on myocardial SPECT images can be created by intense liver uptake (*1,2*). In addition, this artifact is reportedly more prominent when 180° acquisition data, rather than 360° acquisition data, were used for reconstruction (*2*). Although a ^{99m}Tc-tebroxime study suggested that this artifact may occur in the clinical setting (*3*), clinical data focusing on potential significance of this artifactual effect have not yet been available.

Technetium-99m-tetrofosmin was introduced as an alternative myocardial perfusion imaging agent to ^{201}Tl (*4–6*). Tetrofosmin has diagnostic accuracies comparable to ^{201}Tl for detecting coronary artery disease (*7–12*) and for detecting viable myocardium (*13*). The favorable energy emission of ^{99m}Tc (140 keV) reduces photon attenuation compared to ^{201}Tl (70–80 keV). This agent is supplied in kit form and, unlike ^{99m}Tc-sestamibi, does not require heating but only a 15-min incubation at room temperature. Furthermore, its rapid accumulation in the myocardium and relatively rapid clearance from the background organs, compared to ^{99m}Tc-sestamibi, enable imaging as early as 5–15 min after injection, resulting in shorter waiting times for patients (*6,7*). This is important in clinical settings, particularly in patients with suspected acute coronary syndromes and nondiagnostic electrocardiogram, in whom prompt diagnosis for therapeutic decision making is urged (*14–16*). Despite rapid myocardial accumulation, published reports (*6–8*) document that high liver activity still remains at such early time points after injection, which may cause an artifactual defect in the inferior wall due to high hepatic uptake as well as the results of phantom studies (*1,2*).

Theoretically, the myocardial images obtained at early time points after injection of ^{99m}Tc-tetrofosmin should be identical to the delayed images, since this agent shows no significant changes in tracer distribution in the myocardium over time (*6–8,13*). Consequently, we hypothesized that this artifactual effect on myocardial SPECT images could be assessed by comparing early SPECT images to delayed images, in which hepatic uptake would be significantly reduced, and that the absence of significant changes in actual myocardial tracer distribution could be confirmed by the use of planar projection images.

In the present study, we compared early (10-min) and delayed (1-hr) ^{99m}Tc-tetrofosmin myocardial SPECT images in normal volunteers to test the feasibility of early SPECT imaging with the presence of high hepatic activity. In addition, we studied the potential differences of this artifactual effect between 180° and 360° reconstruction data.

MATERIALS AND METHODS

Subjects

We studied 13 male healthy volunteers (age 25–52 yr, mean 33 yr) with no previous history of heart disease. All subjects had a normal physical examination, electrocardiogram and normal chest radiograph. The average height, body weight and thorax girth were 170.5 cm, 72.12 kg and 93.8 cm, respectively. None of the subjects had any other major noncardiac diseases. All subjects gave informed consent form based on the guidelines of the hospital's human clinical study committee before study participation.

Preparation of Technetium-99m-Tetrofosmin

Technetium-99m-tetrofosmin was prepared from a freeze-dried kit by reconstitution with approximately 5 ml of a sterile pertechnetate solution containing 740–1110 MBq ^{99m}Tc.

Myocardial SPECT Image Acquisition

In each subject, 600–740 MBq of ^{99m}Tc-tetrofosmin were intravenously injected at rest; imaging began 10 min and 1 hr after injection. Subjects were instructed to refrain from eating even after injection, since eating is usually prohibited in patients with acute coronary syndromes. Myocardial SPECT imaging was performed using a triple-head SPECT system with low-energy, high-resolution, parallel-hole collimators. The detector system was interfaced to a dedicated nuclear medicine computer. A total of 60 projection images were obtained over 360° in 6° increments, with 20 sec per view. The energy discriminator was centered on 140 keV with a 20% window. The data were recorded in 128 × 128 matrices into the magnetic disk. The projection datasets were smoothed with a two-dimensional Butterworth filter (order 8, cutoff 0.15) and

Received Aug. 10, 1995; revision accepted Dec. 13, 1995.

For correspondence or reprints contact: Ichiro Matsunari, MD, Nuklearmedizinische Klinik und Poliklinik, der Technischen Universität München, Klinikum rechts der Isar, Ismaninger Str. 22, 81675 München, Germany.

reconstructed over 180° (45° RAO to LPO) and over 360° with a ramp filter.

To investigate the effect of prereconstruction filtering, we also tested a higher cutoff frequency of the Butterworth filter (order 8, cutoff 0.20). The reconstructed transaxial images were manually reoriented into short-axis slices (3.2 mm thick) using identical parameters. Then, four serial slices of the SPECT images were added, resulting in 12.8 mm thick. No attenuation correction was performed in the present study. The image data were transferred to Macintosh Quadra based image analysis system for further analysis (*17*).

Data Analysis

Short-axis SPECT images were projected on a monitor screen for visual interpretation by two experienced observers. The cutoff frequency of the Butterworth filter for visual analysis was 0.15 cycles/pixel. The observers knew the reconstruction parameters of the images. Then, the scintigrams were visually scored as normal, equivocal or abnormal. Disagreements in interpretation were resolved by consensus.

Quantitative SPECT data analysis was based on three short-axis slices representing the apical, middle and basal ventricular myocardium. Circumferential profile analysis was performed on an operator-defined region of interest (ROI) around the left ventricular activity of each tomogram. The center of each tomogram was determined and the ROI was automatically subdivided into 128 sectors. The maximum pixel activity within each sector for each image dataset was normalized to the peak activity within the whole heart, which was assigned a value of 100%. The sectors from the middle or basal short-axis slice were averaged into eight myocardial regions, whereas the sectors from the apical short-axis slice were analyzed to assess apical region.

Planar projection image analysis was based on an anterior projection image obtained from each SPECT imaging. Square ROIs were placed on the anterior left ventricular myocardial wall, inferior myocardial wall and the left lobe of liver in the image. Then, liver-to-heart (anterior wall) and anterior-to-inferior ratios were calculated from the counts per pixel in the ROIs.

Statistical Analysis

Data are presented as mean ± s.d. Differences in the mean activities between the early and delayed images were compared using Student's paired or nonpaired t-test. Statistical significance was defined as $p < 0.05$.

RESULTS

Myocardial SPECT Imaging

Visual Analysis. One subject was excluded from further analysis because of high hepatic activity overlapping into the inferior myocardial wall. The remaining 12 subjects had good quality and early and delayed myocardial SPECT images. On the 180° reconstruction data, 4 of 12 subjects (33%) had an abnormal scan with reduced uptake in the inferior wall on the early images. In contrast, only one subject (8%) had an equivocally reduced uptake in the inferior wall on the early 360° SPECT images, which was scored as equivocal. On the delayed images, on the other hand, all subjects had normal 180° and 360° SPECT scans.

Quantitative Analysis

Figure 1 shows the results of quantitative analysis for the 180° reconstruction data. Significant decreases in activities in the early SPECT images compared to those in the delayed images were noted in the inferior regions. The maximum difference between the early and delayed images was seen in the infero-septal region of middle ventricular myocardium. On the other hand, there were no significant differences in the mean activities in the anteroseptal, anterior and anterolateral wall between the early and delayed images.

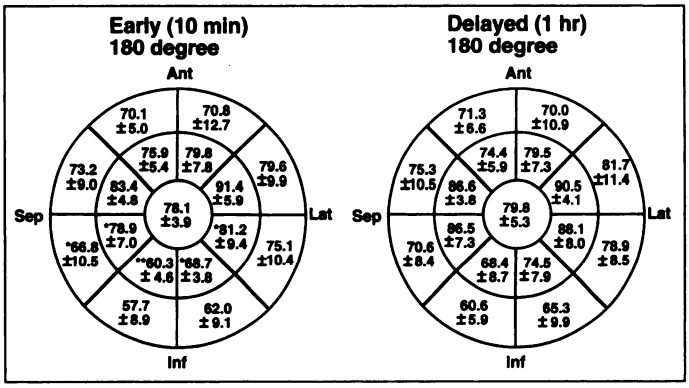

FIGURE 1. Comparison of regional tracer activities between the early (10 min) (left) and delayed (1 hr) (right) myocardial SPECT images (Butterworth filter; order 8, cutoff 0.15) reconstructed from 180° acquisition data. *$p < 0.05$ versus delayed image. **$p < 0.01$ versus delayed image.

Reconstructed data from whole 360° also showed a decrease in the mean activities in the inferior regions (Fig. 2). Nevertheless, the differences were not so significant as those seen in the 180° reconstructed data. Similarly to the results of 180° acquisition data, there were no significant changes in the mean activities in the anteroseptal, anterior and anterolateral wall from the 10-min to 1-hr images.

Figure 3 shows the results of quantitative analysis using a higher cutoff frequency of the prereconstruction filter (Butterworth filter; order 8, cutoff 0.20). The maximum difference in the mean activities between the early and delayed images for the 180° reconstruction data was 8.4 ± 10.5% peak activity, which was comparable to that with the cutoff frequency of 0.15 cycles/pixel (8.1 ± 8.6% of peak activity, ns). Thus, the use of a higher cutoff frequency of the Butterworth filter did not reduce the magnitude of differences in the mean activities between the early and delayed images.

A comparison of early and delayed ^{99m}Tc-tetrofosmin SPECT images reconstructed from 180° and 360° acquisition data is shown in Figure 4.

Planar Projection Imaging

As shown in Table 1, the mean liver-to-heart ratio calculated from planar projection images was high in the early images, and it rapidly declined over time ($p < 0.01$). On the other hand, there were no significant changes in the mean anterior/inferior ratio from the early (10-min) to the delayed (1-hr) images (ns).

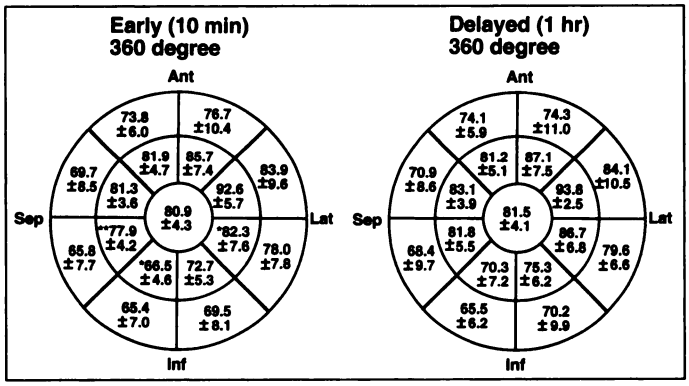

FIGURE 2. Comparison of regional tracer activities between the early (10 min) (left) and delayed (1 hr) (right) myocardial SPECT images (Butterworth filter; order 8, cutoff 0.15) reconstructed from 360° acquisition data. *$p < 0.05$ versus delayed image. **$p < 0.01$ versus delayed image.

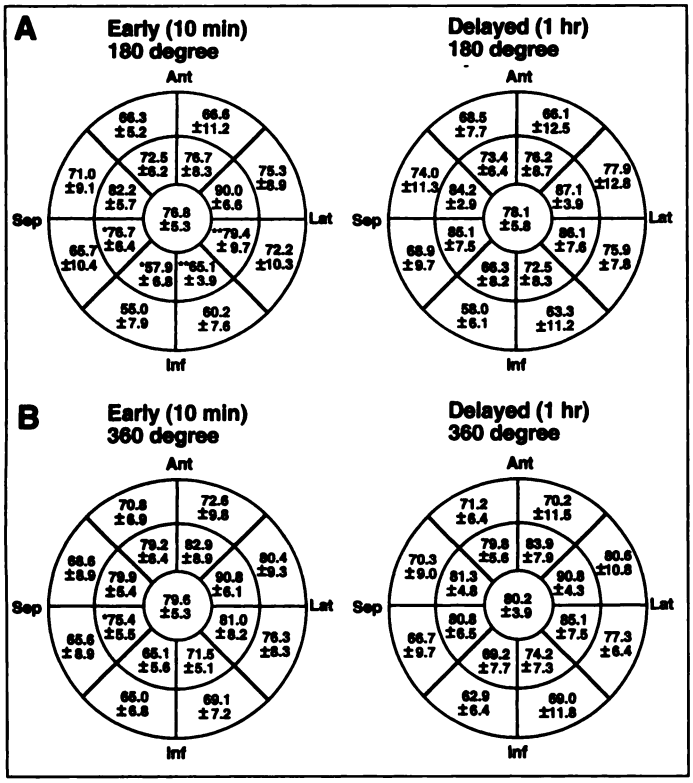

FIGURE 3. Comparison of regional tracer activities between the early and delayed myocardial SPECT images using a higher cutoff frequency of Butterworth filter (order 8, cutoff 0.20) for 180° data (A) and for 360° data (B). *$p < 0.05$ versus delayed image. **$p < 0.01$ versus delayed image.

DISCUSSION

Technetium-99m-tetrofosmin is a newly introduced myocardial perfusion imaging agent (*4–6*). In comparison to ^{99m}Tc-sestamibi, which is the most widely used ^{99m}Tc-based myocardial perfusion imaging tracer, its rapid myocardial uptake and faster clearance from backgrounds allows early imaging after injection (*6–8*). These characteristics are favorable, especially for patients with suspected acute coronary syndromes and a nondiagnostic electrocardiogram, since early diagnosis is needed in such patients for timely therapeutic decision making (*14–16*). Technetium-99m-sestamibi, on the other hand, may require a waiting time of up to 1 hr for imaging.

In our study, however, one subject had high hepatic activity overlapping to the inferior myocardium; therefore, this study was classified as inadequate. Furthermore, we demonstrated that 33% of the subjects showed reduced uptake in the inferior region on the early 180° SPECT image, which was supported by quantitative data that regional tracer activities in the inferior regions on the early SPECT images, were significantly reduced compared to those in the delayed SPECT images especially when the images were reconstructed from 180° acquisition data. There were no significant changes, on the other hand, in the mean anterior-to-inferior ratio between the early and delayed planar projection images, indicating that this transitional reduced activity in the inferior regions observed in the early SPECT images was not likely to reflect truly reduced tracer activity in the inferior myocardium, but might reflect some artifactual effects.

Potential Mechanisms for Artifact

Possibly, the reduced activities in the inferior regions on the early SPECT images could be explained by the liver-to-heart artifact due to intense tracer uptake in the liver (*1,2*). The presence of high liver activity adjacent to the inferior wall results from oversubtraction of activity from the inferior wall.

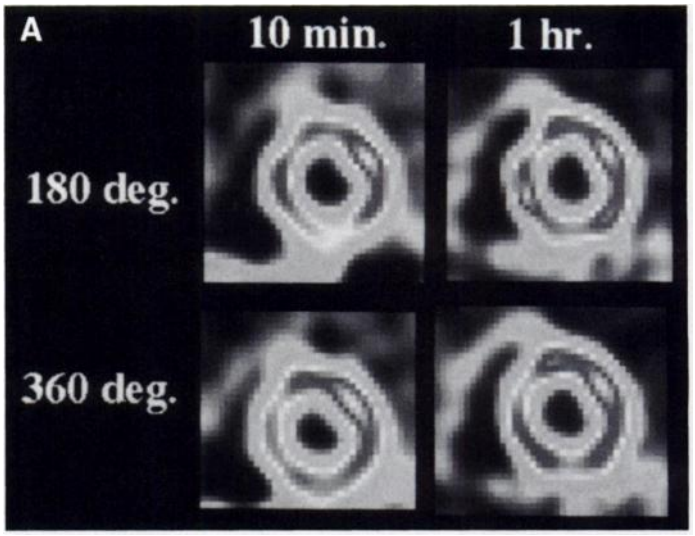

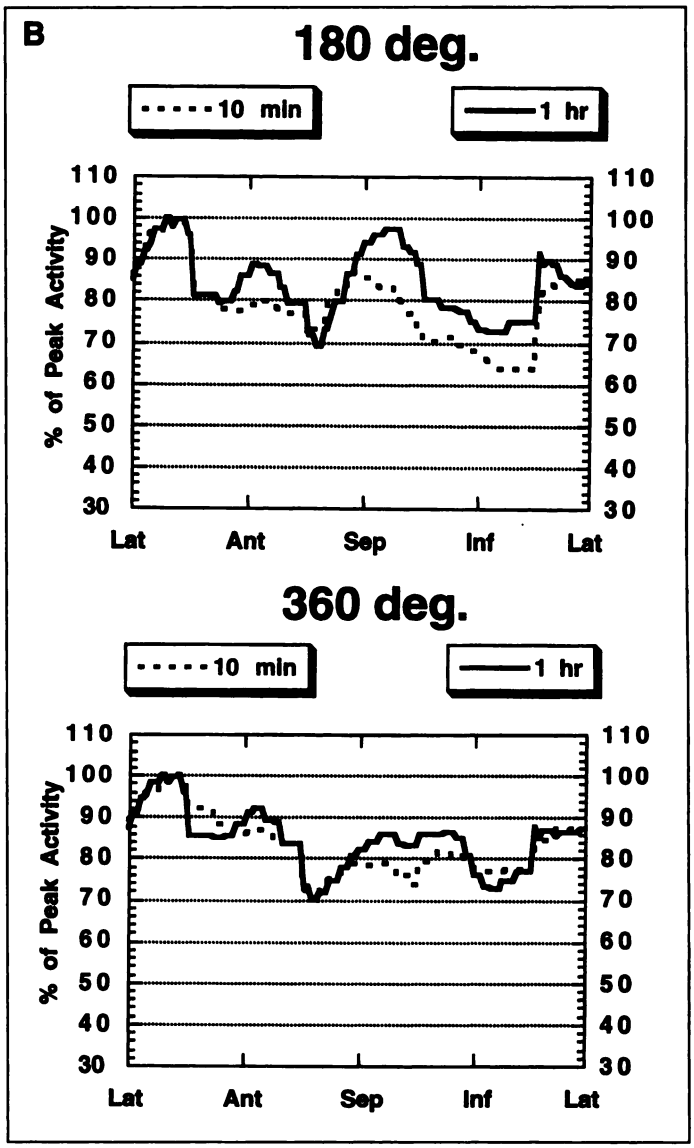

FIGURE 4. A representative case example comparing the early (10 min) and delayed (1 hr) SPECT images for 180° and 360° reconstruction data (Butterworth filter; order 8, cutoff 0.15) (A) and corresponding circumferential profile curves (B).

Actually, the liver-to-heart ratio, derived from planar projection images on the early images, was remarkably high (1.72 ± 0.47) compared to that on the delayed images (0.59 ± 0.15).

TABLE 1
Count Ratios Calculated from Planar Images

	Early (10 min)	Delayed (1 h)
Anterior/Inferior Ratio	0.97 ± 0.04*	0.99 ± 0.04
Liver/Heart Ratio	1.72 ± 0.47†	0.59 ± 0.15

*ns versus delayed image.
†$p < 0.01$ versus delayed image.

In addition to the level of hepatic activity relative to the myocardium, the distance between the liver and heart, which may vary considerably among patients, is also an important factor (*2*). Therefore, this artifact is likely to be extremely patient-dependent and its severity is hard to predict. Delayed imaging, however, will clearly reduce the artifactual effect, although the optimal time is not determined in this study since we mainly focused on determining whether the artifactual defect, can occur on early SPECT images. It should also be noted that our results do not directly apply to exercise stress studies because exercise stress is well known to reduce hepatic tracer uptake relative to the heart.

Comparison of 180° and 360° Reconstruction

In the current study, the decrease in the inferior wall activity on the early SPECT images was more prominent when the images were reconstructed from 180° acquisition data and, by visual analysis, only one subject had an equivocally reduced uptake in the inferior wall on the early 360° SPECT images. This is consistent with the phantom study that showed the 360° reconstruction reduces the differences in attenuation between the different projections therefore reducing the reconstruction artifacts (*2*). Although a 360° reconstruction appears to be more favorable for early imaging, the artifactual effect may not be fully eliminated.

Effect of Different Prereconstruction Filtering Parameters

Germano et al. (*1*) showed that the use of high cutoff frequency of the prereconstruction filter resulted in reduced severity of this artifact. In the present study, however, this was not the case and the use of a higher cutoff frequency of Butterworth filter (order 8, cutoff 0.20) did not reduce the magnitude of the artifact. It may be argued that the use of a much higher frequency of the Butterworth filter (e.g., 0.30) could have reduced the severity of the artifact. In this study, however, we did not test a higher cutoff frequency than 0.20. This reflects routine clinical practice in our laboratory and, in our experience, the use of such a high cutoff frequency of the prereconstruction filter often results in images of unacceptably poor quality even with ^{99m}Tc-based myocardial imaging agent.

Comparison to Phantom Studies

The reduced inferior wall activity observed in our study appears to be less significant than those reported in phantom studies (*1,2*). This could partly be explained by the differences between the real human thorax and the simplified phantoms used in their studies. The phantom studies did not simulate complicated body structures including lung, spine and chest wall, since they purely focused on investigating relationships between the liver and heart (*1,2*). The reduced activity, however, in the inferior wall on the early SPECT images in the present study is visually identifiable as a decreased perfusion, especially when 180° acquisition data are used for reconstruction (Fig. 4), suggesting that a misinterpretation of the images can occur due to this artifactual effect.

Potential Limitations

Attenuation correction was not performed in this study. With the attenuation correction, the artifactual defect observed in the early SPECT images could be considerably canceled out (*2*). Nevertheless, although approaches have been published with attenuation correction (*18,19*), no widely accepted and prospectively validated quantitative approach is currently available for the evaluation of clinical SPECT studies. Image interpretation without attenuation correction is currently used in most clinical settings for analysis of SPECT studies.

Our study is based upon a relatively small number of subjects. Therefore, although our study clearly shows that this artifact is clinically relevant, further studies involving a larger number of subjects may be needed before a definitive statement with respect to the exact frequency of this artifact is drawn.

CONCLUSION

In patients with suspected acute coronary syndromes, prompt diagnosis is urged for timely therapeutic decision making. In this regard, ^{99m}Tc-tetrofosmin appears to be attractive because of its rapid accumulation in the myocardium with rapid clearance from background organs, which may result in shorter waiting time. Our results, however, did show that one subject had an inadequate study because of high hepatic activity directly affecting the inferior myocardium. Furthermore, resting ^{99m}Tc-tetrofosmin myocardial SPECT images at 10 min after injection may show an artifactual defect in the inferior wall even without hepatic activity overlapping into the myocardium, particularly when the images are reconstructed from the 180° acquisition data. Therefore, it would be best to perform late imaging in patients with suspected coronary artery disease using ^{99m}Tc-tetrofosmin.

ACKNOWLEDGMENTS

We thank Dr. S. Ziegler and Mr. G. Böning of the Nuklearmedizinische Klinik und Poliklinik der Technischen Universität München for their suggestive comments.

REFERENCES

1. Germano G, Chua T, Areeda J, Kiat H, Berman D. Hepatic uptake creates artificial defects in ^{99m}Tc myocardial SPECT images: a quantitative phantom analysis. *J Nucl Med* 1994;35:356–359.
2. Nuyts J, Dupont P, den Maegdenbergh VV, Vleugels S, Suetens P, Mortelmans L. A study of liver-heart artifact in emission tomography. *J Nucl Med* 1995;36:133–139.
3. Chua T, Kiat H, Germano G, et al. Rapid back to back adenosine stress/rest technetium-99m-tebroxime myocardial perfusion SPECT using a triple-detector camera. *J Nucl Med* 1993;34:1485–1493.
4. Higley B, Smith FW, Smith T, et al. Technetium-99m-1, 2-bis[bis(2-ethoxyethyl) phosphino]ethane: human biodistribution, dosimetry and safety of a new myocardial perfusion imaging agent. *J Nucl Med* 1993;34:30–38.
5. Kelly JD, Forster AM, Higley B, et al. Technetium-99m-tetrofosmin as a new radiopharmaceutical for myocardial perfusion imaging. *J Nucl Med* 1993;34:222–227.
6. Jain D, Wackers FJT, Mattera J, McMahon M, Sinusas AJ, Zaret BL. Biokinetics of technetium-99m-tetrofosmin: myocardial perfusion imaging agent: Implications for a one-day imaging protocol. *J Nucl Med* 1993;34:1254–1259.
7. Sridhara BS, Braat S, Rigo P, Itti R, Cload P, Lahiri A. Comparison of myocardial perfusion imaging with technetium-99m-tetrofosmin versus thallium-201 in coronary artery disease. *Am J Cardiol* 1993;72:1015–1019.
8. Nakajima K, Taki J, Shuke N, Bunko H, Takata S, Hisada K. Myocardial perfusion imaging and dynamic analysis with technetium-99m-tetrofosmin. *J Nucl Med* 1993; 34:1478–1484.
9. Rigo P, Leclercq B, Itti R, Lahiri A, Braat S. Technetium-99m-tetrofosmin myocardial imaging: a comparison with thallium-201 and angiography. *J Nucl Med* 1994;35:587–593.
10. Tamaki N, Takahashi N, Kawamoto M, et al. Myocardial tomography using technetium-99m-tetrofosmin to evaluate coronary artery disease. *J Nucl Med* 1994;35:594–600.
11. Hendel RC, Parker MA, Wackers FJT, Rigo P, Lahiri A, Zaret BL. Reduced variability of interpretation and improved image quality with a technetium-99m myocardial perfusion agent: comparison of thallium-201 and technetium-99m-labeled tetrofosmin. *J Nucl Cardiol* 1994;1:509–514.
12. Zaret BL, Rigo P, Wackers FJT, et al. Myocardial perfusion imaging with ^{99m}Tc-tetrofosmin: comparison to ^{201}Tl imaging and coronary angiography in a phase III multicenter trial. *Circulation* 1995;91:313–319.
13. Matsunari I, Fujino S, Taki J, et al. Myocardial viability assessment with technetium-99m-tetrofosmin and thallium-201 reinjection in coronary artery disease. *J Nucl Med* 1995;36:1961–1967.

14. Hilton TC, Thompson RC, Williams HJ, Seiylors R, Fulmer H, Stowers SA. Technetium-99m-sestamibi myocardial perfusion imaging in the emergency room evaluation of chest pain. *J Am Coll Cardiol* 1994;23:1016–1022.
15. Cuocolo A, Soricelli A, Nicolai E, et al. Technetium-99m-tetrofosmin regional myocardial uptake at rest: relation to severity of coronary artery stenosis in previous myocardial infarction. *J Nucl Med* 1995;36:907–913.
16. Stowers SA. Myocardial perfusion scintigraphy for assessment of acute ischemic syndromes: can we seize the moment? *J Nucl Cardiol* 1995;2:274–277.
17. Matsunari I. Personal computer-based integrated image analysis system interfaced to a SPECT system. *Medical Review (Toshiba) (in Japanese)* 1994:18–2:12–16.
18. Ficaro EP, Fessler JA, Ackermann RJ, Rogers WL, Corbett JR, Schwaiger M. Simultaneous transmission emission thallium-201 cardiac SPECT: effect of attenuation correction on myocardial tracer distribution. *J Nucl Med* 1995;36:921–931.
19. Bacharach SL, Buvat I. Attenuation correction in cardiac positron emission tomography and single-photon emission tomography. *J Nucl Cardiol* 1995;2:246–255.Q1: Au: Cite affilliation for Ziegler and Bonning in Acknowledgments in English.

Reproducibility of Measurements of Regional Resting and Hyperemic Myocardial Blood Flow Assessed with PET

Shigeki Nagamachi, Johannes Czernin, Anatole S. Kim, Karl T. Sun, Morten Böttcher, Michael E. Phelps and Heinrich R. Schelbert

Department of Molecular and Medical Pharmacology, Division of Nuclear Medicine, UCLA School of Medicine; and Laboratory of Structural Biology and Molecular Medicine, University of California, Los Angeles, California

PET with ^{13}N-ammonia permits the noninvasive quantification of myocardial blood flow (MBF) in humans. The present study was done to assess the reproducibility of quantitative blood flow measurements at rest and during pharmacologically induced hyperemia in healthy individuals. **Methods:** Thirty healthy volunteers (26 men, 4 women) were studied. Paired measurements of MBF at rest (n = 21), during adenosine (n = 15) and during dipyridamole (n = 7) were performed using a two-compartment model for ^{13}N-ammonia PET. The mean difference between baseline and follow-up blood flow (% difference) was calculated to assess reproducibility. **Results:** No significant difference was observed between resting blood flow at baseline or follow-up (15.8% ± 15.8%; p = ns). Baseline and follow-up resting blood flow were linearly correlated (r = 0.63, p < 0.005). Normalization of resting blood flow to the rate pressure product improved the reproducibility significantly (15.8% ± 15.8% versus 10.1% ± 10.5%, p < 0.05). Baseline and follow-up hyperemic myocardial blood flow did not differ (11.8% ± 9.4%; p = ns) and were linearly correlated (r = 0.69, p < 0.0005). **Conclusion:** MBF at rest can be measured reproducibly with ^{13}N-ammonia PET. The individual response to pharmacologic stress appears to be relatively consistent. Thus, serial blood flow measurements with ^{13}N-ammonia PET can be used to quantify the effect of various interventions on MBF and vasodilatory reserve.

Key Words: myocardial blood flow; pharmacologic stress; PET

J Nucl Med 1996; 37:1626–1631

PET with either ^{13}N-ammonia or ^{15}O-water and an appropriate tracer compartmental model allows for noninvasive quantification of myocardial blood flow (MBF) (*1–7*). Such measurements have been used in healthy volunteers (*1–3,8,9*), patients with coronary artery disease (*3,10,11*) and other cardiac diseases (*12,13*). Additionally, these measurements have been used to assess the effect of pharmacologic intervention (*14*), cardiovascular conditioning (*15*), coronary angioplasty (*16,17*) and immunosuppressive treatment on rejecting heart transplant on MBF (*18*).

The reproducibility of regional MBF measurements with ^{13}N-ammonia and dynamic PET, however, has yet to be extensively examined (*19*). Establishing the reproducibility of this method would be particularly important for serial PET measurements of MBF after pharmacologic or therapeutic interventions.

Thus, the aim of the current study was to determine the reproducibility of ^{13}N-ammonia PET measurements of MBF at rest and during pharmacologically induced hyperemia in a group of healthy individuals.

MATERIALS AND METHODS

Subjects

Thirty healthy volunteers (26 men, 4 women) with a mean age of 33.7 ± 15.4 yr and a low likelihood for coronary artery disease were included in this study (*20*). None of the participants were taking any medication and all refrained from caffeine intake 24 hr before the PET study (*21*). Each participant signed an informed consent form approved by the UCLA Human Subject Protection Committee.

Study Protocol

Paired resting MBF studies were performed in eight individuals within the same day. Also within the same day, nine other participants had paired hyperemic blood flow studies during intravenous adenosine. Lastly, both paired resting and paired hyperemic blood flow studies (adenosine; n = 6 or dipyridamole; n = 7) were obtained in the 13 remaining participants at an average time interval of 26.5 ± 18.9 days.

Adenosine and dipyridamole induce comparable degrees of myocardial hyperemia (*9*). The relatively long half-life of dipyridamole (30 min), however, precludes serial hyperemic blood flow studies within the same day (*22*). Adenosine has a short half-life of < 5 sec (*23*). Therefore, the reproducibility of hyperemic blood flow within the same day was tested with adenosine while the reproducibility of hyperemic blood flow measurements on separate occasions was assessed with dipyridamole.

Adenosine was infused intravenously at a rate of 140 μg/kg for 6 min. Three minutes after the start of the adenosine infusion, 370–555 MBq of ^{13}N-ammonia were injected intravenously over 30 sec while the serial PET image acquisition was started. For dipyridamole induced hyperemia, dipyridamole (0.56 mg/kg) was infused intravenously over 4 min (*24*). Four minutes later, 370–555 MBq of ^{13}N-ammonia was injected over 30 sec and the serial

Received Aug. 18, 1995; revision accepted Dec. 13, 1995.
For correspondence or reprints contact: Johannes Czernin, MD, Department of Molecular and Medical Pharmacology, B2-085 J CHS, 10833 Le Conte Avenue University of California, Los Angeles, CA 90024-6948.